Folia Hort. 34(1) (2022): 105–124

DOI: 10.2478/fhort-2022-0009

FOLIA HORTICULTURAE

Published by the Polish Society for Horticultural Science since 1989

ORIGINAL ARTICLE | Open access | http://www.foliahort.ogr.ur.krakow.pl

Zn^{2+} induces changes in activities of mitochondrial respiratory chain complexes and emissions of floral volatiles in *Dendrobium huoshanense*

***Wangsheng Zhu*[1,*], *Jun Dai*[1], *Jiahong Wang*[2]**

[1] Engineering Technology Research Center for Plant Cell of Anhui Province, West Anhui University, Lu'an, China
[2] Department of Food Science and Technology, College of Light Industry and Food Engineering, Nanjing Forestry University, Nanjing, China

ABSTRACT

In recent years, there has been increasing interest in floral volatiles due to their important function in reproduction, self-protection and so on. Although some progress was made on deciphering emissions of floral volatiles and on related mechanisms under a variety of environmental factors, the effects of Zn^{2+} concentrations on mitochondrial function and floral volatile emissions are yet to be revealed. *Dendrobium huoshanense* petals were used as materials and were treated with a 0–8 mM $ZnSO_4$ solution. Intracellular Zn^{2+} concentrations were evaluated by the fluorescent dye method and atomic absorption method. Mitochondrial respiratory chain complex activities and the precursor and ATP contents were determined by the biochemical method. Floral volatile components were analyzed by the gas chromatograph-mass spectrometer (GC-MS). The results indicated that $ZnSO_4$ application significantly increased intracellular Zn^{2+} concentrations. Elevated intracellular Zn^{2+} concentrations differently affected mitochondrial respiratory chain complex activities, precursor and adenosine triphosphate (ATP) productions and floral volatile emissions. Moreover, positive correlations exist among the activities of mitochondrial respiratory chain complexes, productions of precursors and ATP and emissions of floral volatiles. It is concluded that Zn^{2+} concentrations induce the activity changes of mitochondrial respiratory chain complexes, especially complex II and V, which promote or inhibit the emissions of floral volatiles by affecting the precursor and ATP levels that are closely related to the production of terpenoids, benzoids and fatty acid derivatives. The research will contribute to understanding the relationship between Zn^{2+} concentrations and floral volatile emissions from the perspective of mitochondrial function.

Keywords: ATP, *D. huoshanense*, floral volatiles, mitochondrial respiratory chain complexes, precursors, Zn^{2+} *concentrations*

INTRODUCTION

Floral volatiles are a class of low-molecular-weight (~100–200 Da) lipophilic compounds with high vapour pressure (Adebesin et al., 2017). These compounds play an important role in attracting pollinators and seed dispersers, defending against herbivores and pathogens from above and below the ground and transmitting signals between plants. These are also beneficial to floriculture, cosmetic, flavour and scent industries (Muhlemann et al., 2014; Barman and Mitra, 2019; Campbell et al., 2019; Cordeiro et al., 2019). Environmental factors have been shown to influence the category and quantity of floral volatiles (Hu et al., 2015; Chuang et al., 2017; Fu et al., 2017; Qi et al., 2020). Mineral elements, being one of the most essential environmental parameters for plants, have a significant impact on floral volatile emissions. For example, Ca^{2+} contributes to the

*Corresponding author.
e-mail: zhuws@wxc.edu.cn (Wangsheng Zhu).

synthesis and emission of monoterpenes in the flower of *Lilium* "Siberia" (Hu et al., 2015). At present, research on environmental factors, including mineral elements affecting floral volatile emissions, is mainly focussed on the plant circadian clock, terpene synthase (TPS) and phenylalanine ammonia-lyase (PAL) activities, related TPS and PAL gene expressions, etc. (Bera et al., 2017; Chuang et al., 2017; Huang et al., 2018; Abbas et al., 2019). However, there are limited reports on the relationship between Zn^{2+} and floral volatile emissions from the perspective of the mitochondrial function of plant cells.

Floral volatiles are mainly composed of terpenoids, benzoids and fatty acid derivatives (Han et al., 2019). To date, at least 1,700 kinds of floral volatile compounds have been identified (Mohd-Hairul et al., 2010). Their syntheses and emissions are directly or indirectly associated with the tricarboxylic acid (TCA) cycle and oxidative phosphorylation in mitochondria. First, the precursor of floral volatiles is mainly derived from metabolism intermediates in the TCA cycle. For instance, the precursors of terpenoids are isopentenyl pyrophosphate (IPP) and dimethylallyl pyrophosphate (DMAPP), which originate from the acetyl-coenzyme A and acetylformic acid intermediates in the TCA cycle. IPP and DMAPP are then catalysed by geranyl diphosphate synthase (GPS) and metabolised to monoterpenes, diterpenes, tetraterpenes and derived compounds; these are also catalysed by farnesyl diphosphate synthase (FPS) and metabolised to sesquiterpenes, triterpenes and their derivatives. Similarly, the precursor of benzoids is phenylalanine (Phe), which is related to the fumaric acid intermediate in the TCA cycle. Phe is then catalysed by PAL and metabolised to phenylpropanoids, benzenoids and phenylpropanoid-related compounds (van Schie et al., 2006). The precursors of fatty acid derivatives are linoleic acid (LA) and linolenic acid (LNA), which are related to acetyl-coenzyme A intermediate in the TCA cycle. LA and LNA are then catalysed by a lipoxygenase (LOX) and metabolised to volatile alcohols, esters, aldehydes and so on (Muhlemann et al., 2014). Then, the oxidative phosphorylation in the inner membrane of mitochondria can provide energy for synthesis and emissions of floral volatiles. Recent studies have shown that energy from adenosine triphosphate-binding cassette (ABC) transporter promotes the emission of floral volatiles in *Petunia hybrida* (Adebesin et al., 2017). Thus, it is theoretically possible to alter the production rate of precursors and adenosine triphosphate (ATP) and emissions of floral volatiles by regulating the TCA cycle and oxidative phosphorylation in mitochondria.

Mitochondrial respiratory chain complexes (I, II, III, IV and V), also known as respiratory chain complex enzymes, are an important indicator of mitochondrial function. They are closely linked with the function of the TCA cycle and oxidative phosphorylation in mitochondria (Heidarvand et al., 2017; Cogliati et al., 2018; Fedor and Hirst, 2018). Zinc (Zn), as an important micronutrient, plays a variety of roles in various biochemical processes, including enzyme activation, respiration action, carbon (C) and nitrogen (N) metabolism, flower development and intracellular signal transduction, etc. (Rezaeieh et al., 2016; Farooq et al., 2018; Olechnowicz et al., 2018; Shoaib et al., 2021). However, the low solubility of Zn in the soil often leads to Zn deficiency in crops. Foliar fertilisation of Zn is an effective method to increase Zn concentration in plants (Bautista-Diaz et al., 2021). The flower has also been shown to absorb Zn directly. A study has reported that flower buds of *Hibiscus rosa-sinensis* can absorb Zn^{2+} (Sawidis et al., 2014). Based on the above-mentioned functions of the mitochondrial respiratory chain complexes and the characteristics of Zn, the relationships between Zn^{2+} and mitochondrial respiratory chain complex activities and floral volatile emissions are conceived as follows: (1) how do the Zn^{2+} concentrations affect respiratory chain complex activities? (2) How do precursors, ATP production rates and floral volatile emissions respond to alterations of respiratory chain complex activities?

Dendrobium species (Orchidaceae) are very popular since ancient times because of their important ornamental and health values. In China, more than 70 species of *Dendrobium* spp. are distributed. Most of them are abundant in medicinal ingredients such as polysaccharides, alkaloids and other biologically active substances, and their flowers are fragrant (Jin et al., 2016). As early as the Han Dynasty, they were first mentioned in the "*Sheng Nong's Herbal Classic*" (a Chinese ancient book), where they were classified as the superior medicinal articles (Yuan et al., 2019; Chen et al., 2020). Since then, as traditional valuable Chinese herbs and ornamental plants, wild *Dendrobium* species such as *Dendrobium huoshanense, Dendrobium officinale* and *Dendrobium nobile* were heavily mined and nearly depleted (Zheng et al., 2018). Nowadays, they are being protected and propagated. Modern pharmaceutical research has indicated that *D. huoshanense* has antioxidant, anticancer and anti-diabetes effects. It has been used to treat a wide range of symptoms, including throat inflammation, immunodeficiency, superficial gastritis, chronic gastritis and weak eyesight (Yuan et al., 2019; Chen et al., 2020). Their flowers contain various volatile oils and non-volatile organic compounds, including terpenes, soluble sugars, free amino acids, and phenolic compounds, and are important raw materials for functional foods.

Given the flower's great potential to be developed as functional foods, including essential oils, tea products, etc., *D. huoshanense* cultivation is increasingly expanding in China. In this study, we applied a 0–8 mM $ZnSO_4$ solution to investigate the change of intracellular Zn^{2+} concentrations in *D. huoshanense* petals. We focussed on whether intracellular Zn^{2+} concentrations alter the activities of mitochondrial respiratory chain complexes and subsequent flower volatile emissions. Further, we focussed on whether there is a correlation between the changes in the activities of the mitochondrial respiratory chain complexes and emissions of flower volatiles. The purpose was to unveil the relation between Zn^{2+} and

floral volatile emissions from the perspective of the activities of mitochondrial respiratory chain complexes.

MATERIALS AND METHODS

Plant materials and growth conditions

The experimental plant material was a 3-year-old *D. huoshanense*, grown in the greenhouse (Figures 1A–1D) in the botanical garden of West Anhui University, Lu'an City, Anhui Province, China. The greenhouse was covered with the sunshade net in 70% light transmittance of natural light, on the roof, and was automatically controlled in 40%–60% of humidity when the diurnal temperature was from −5 ℃ to 40 ℃. The culture medium was pine barks, which were naturally fermented after being piled on the ground.

Experimental treatments and sample collections

D. huoshanense plants at a full-bloom stage were randomly divided into four groups: three treatment groups and one control group. Each group contains 10 *D. huoshanense* plants. The plant's petals of three different treatment groups were sprayed with 50 mL $ZnSO_4$ solution in 2 mM, 4 mM and 8 mM concentrations, respectively. The control group's petals were treated with the same volume of distilled water. Each processing was set to three repetitions. A total of 600 mL of $ZnSO_4$ solution was applied, and 120 *D. huoshanense* plants were examined. The spraying of the $ZnSO_4$ solution did not cause obvious visual changes to the petals. At 6 h after the treatment, sufficient fresh petals were collected to prepare protoplast and analyse intracellular Zn^{2+} concentrations. Furthermore, at 6 h,

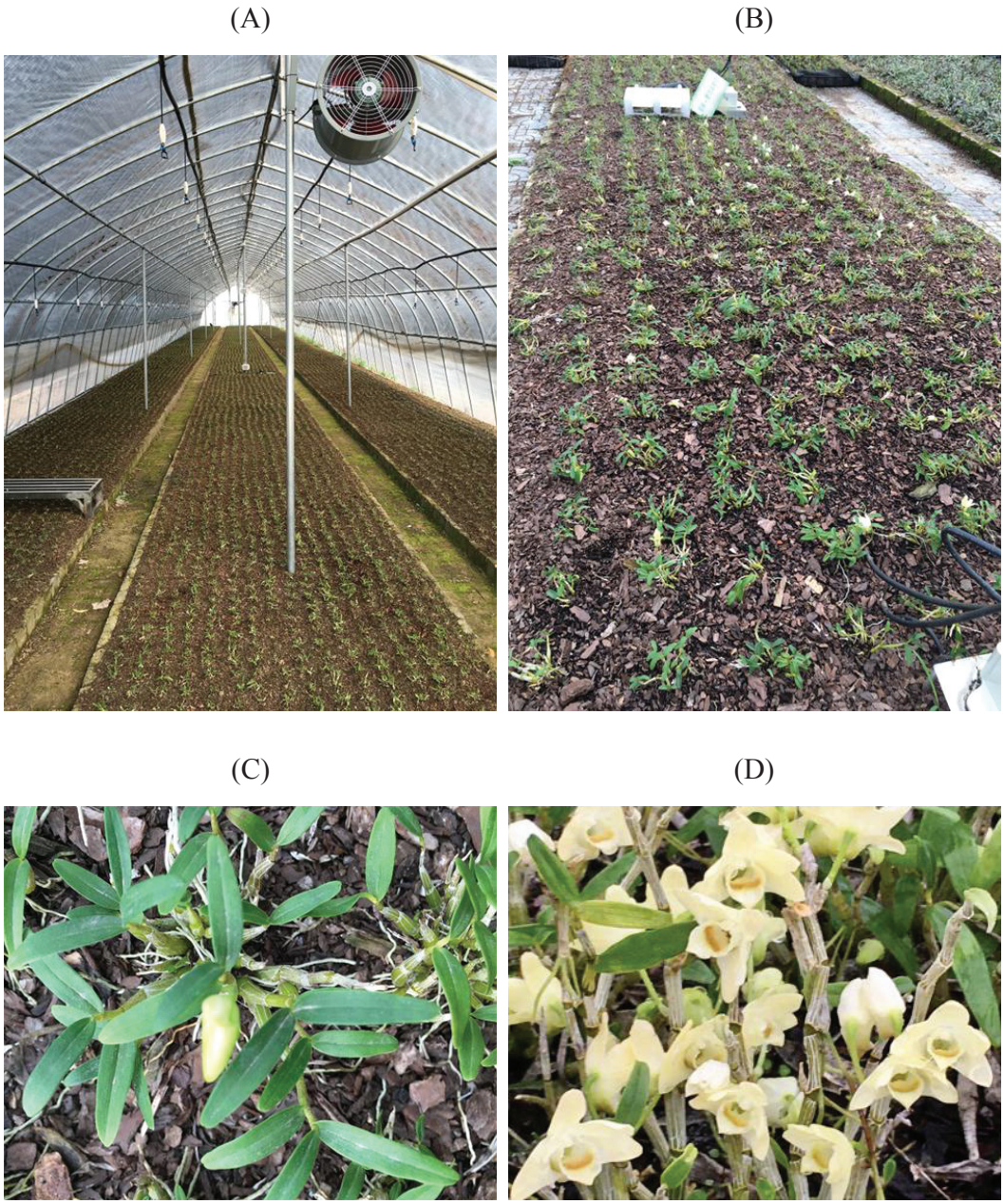

Figure 1. Population (A,B), plant (C) and flower (D) of *D. huoshanense* in the greenhouse.

9 h and 12 h, petals of 5 g were collected from every experiment group and were cut into pieces to put into a 20-mL headspace (HS) bottle. Subsequently, 5 g of anhydrous sodium sulphate and 10 µL of 0.05 mg · mL^{-1} 2-nonanone were added into each bottle as the internal standards for chromatographic analysis, and the bottle was sealed with an attached cap. At every above-mentioned moment, a sufficient number of petals collected were instantly frozen in liquid nitrogen and stored at −80 ℃ for further use, including the analysis of respiratory chain complex activities and the precursor and ATP levels (at 6 h, 9 h and 12 h after the treatment).

Evaluation of intracellular Zn^{2+} concentrations

To comprehensively assess the change of intracellular Zn^{2+} concentrations, we determined the intracellular fluorescence intensity of Zn^{2+} and zinc concentrations in petals. Then, 10 g of fresh petals were cut into 1-mm pieces. The petal pieces were used to prepare cell protoplast suspension by the enzymatic hydrolysis method (Guilley and Hahne, 1989). Then, 10 µL fluorescent dye ZnAF-2F DA (Chemodex Ltd., St. Gallen, Switzerland) was added to 10 mL prepared protoplast suspension and was incubated in a petri dish under room temperature and dark conditions for 30 min. After the incubation, a fluorescence confocal microscope (FluoView FV1200, Olympus, Tokyo, Japan) was used for the observation of fluorescence intensity. Representative photos (60×) were taken, and the fluorescence intensity was analysed with Image J software. Zn^{2+} fluorescence intensity value was the mean of nine fluorescence measurements of three photos/protoplasts. Fluorescence intensity measurement of each time was calculated using the ratio of "integrated density/area". The "area" was the region occupied by a specific number of protoplasts measured in the image, while "integrated density" was the sum of fluorescence intensities in the region. As for zinc concentrations, sufficient petals were ground and passed through a No. 40 sieve. Next, 50 g of the test sample was taken and carbonised into powder. Then, the powder was heated in a muffle furnace until it turned ash grey. According to the method described by Ashok Kumar et al. (2013), zinc concentrations were determined by the atomic absorption spectrophotometer (AA-6000).

Mitochondrial purification and activity determination of respiratory chain complexes

Thirty grams of petals were cut into pieces; then, 120 mL of the extraction medium was added and immediately ground in a mortar to homogenate under ice bath conditions. The above extraction medium consisted of 20 mM HEPES-Tris (pH 7.5), 0.3 M sucrose, 1 mM 1,4-dithioerythritol (DTE), 5 mM sodium-ethylenediaminetetraacetic acid (Na-EDTA), 0.3% (w/v) bovine serum albumin (BSA) and 0.6% (w/v) polyvinylpolypyrrolidone (PVPP). After homogenising, the mitochondrial components were sequentially extracted and purified by differential centrifugation and Percoll density gradient centrifugation according to the method of Petrussa et al. (2008). The final purified material was resuspended in suspension [20 mM HEPES-Tris, pH 7.5, 0.1% (w/v) defatted BSA, 0.3 M sucrose]. The concentration of mitochondrial protein was monitored by the coomassie brilliant blue method and adjusted to 0.5 mg · mL^{-1}, and the protein was then stored on ice.

The activity of complex I (NADH-ubiquinone oxidoreductase) was evaluated by measuring the NADH oxidation rate according to the method described by Estornell et al. (Estornell et al., 1993; Srivastava et al., 2017). The reaction was started by adding the appropriate amount of buffer to 50 µL of the protein sample. The buffer consisted of 100 mM coenzyme Q1, 10 mM Tris-HCl (pH 7.4), 1 mM EDTA, 2 mM N-ethylmaleimide (NEM), 2 mM potassium cyanide (KCN) and 50 mM KCl. The absorbance change of the reaction solution was measured with a spectrophotometer (UV-5100) at 340 nm. The activities of complex II (succinate dehydrogenase), III (ubiquinol cytochrome c reduction) and IV (cytochrome c oxidase) were measured according to the method described by Srivastava et al. (Srivastava et al., 2017; Zamiri et al., 2017). Briefly, the activity of complex II was determined by reducing 2,6-dichlorophenolindophenol (DCPI) with phenazine methyl sulphate (PMS). A 50-µL protein sample was taken and added to a medium containing 100-µM PMS, 50-mM KH_2PO_4 (pH 7.5), 16-mM sodium succinate and 1.5-mM KCN. After 3-min incubation at 37°C, 100 µM of DCPI was added to measure the difference in absorbance at 600 nm. The activity of complex III was determined by measuring the absorbance of cytochrome C at 550 nm. Approximately, 50 µL of the sample was added to the reaction medium containing 35 mM KH_2PO_4 (pH 7.5), 125 mM oxidized cytochrome C, 10 µg · mL^{-1} rotenone, 5 mM $MgCl_2$, 1.8 mM KCN and 2.5 mg · mL^{-1} BSA. After 30 s of incubation at 37 °C, the reaction was initiated by adding 31.8 µM reduced ubiquinone 2. Absorbance with and without 10 µg · mL^{-1} antimycin A was monitored. The activity of complex IV was determined by measuring the oxidation rate of cytochrome C. The reaction was performed using 50 µL of the protein sample in 50 mM phosphate buffer (7.4 pH). Absorbance was monitored at 550 nm with or without 2 mM KCN. Regarding complex V (ATP synthase), its activity was determined according to the report of Zamiri et al. (2017). Approximately, 50 µL of the protein sample was added to a medium containing 50 mM Tris (pH 8.0), 50 mM KCl, 20 mM $MgCl_2$, 15 µM carbonyl cyanide m-chlorophenylhydrazone (CCCP), 10 mM phosphoenolpyruvate, 5 mM antimycin A, 2.5 mM ATP, 5 mg · mL^{-1} BSA, 1 mM NADH, 20 U of pyruvate kinase and 20 U of lactate dehydrogenase. After 30 s of incubation at 37 °C, a reaction was performed in the presence and absence of 3 µM oligomycin. Absorbance was monitored at 340 nm.

Measurement of precursor and ATP contents

Depending on the method described by Zhou et al. (2013), IPP and DMAPP contents were estimated by

measuring the isoprene production rate. Briefly, fresh petals were ground and divided into two halves directly into 5 mL test tubes. Ice cold extraction buffer (100 mM NH_4HCO_3:isopropanol:acetonitrile = 1:1:3) was added to the tubes to extract the powder. The extracts were centrifuged at 4°C for 15 min. Supernatants were transferred and dried. Then, isoprene synthase and/or isopentenyl diphosphate isomerase was added to initiate the reaction. DMADP content was quantified by converting it to isoprene using isoprene synthase. The total content of IPP plus DMADP was measured by including isopentenyl diphosphate isomerase in the reaction mixtures. IPP content was determined according to the difference between the total measurement and the DMADP measurement. Isoprene emission from the reaction was measured with a fast isoprene sensor (LY500-C5H8). Phe content was established by referring to the method of Li et al. (2017). Petal samples were ground and extracted with 1.0 mL of extraction liquid (chloroform: methanol, 1:3, v:v). Subsequently, the extracts were centrifuged at 4 °C for 10 min. The supernatant was transferred into a glass vial and dried in a vacuum chamber at 30 °C. Then, samples were derivatised with N-trimethylsilyl-N-methyl trifluoroacetamide at 70 °C for 1 h, and the Phe content was determined using gas chromatography. The operating conditions of gas chromatography (ThermoFisher Trace) were as follows: (1) the carrier gas was helium, with a flow rate of 1 mL · min^{-1}, (2) the injector and detector temperatures were both set at 280 ℃ and (3) the column temperature was kept at 70 ℃ for the first 2 min and then increased to 300 ℃ at a rate of 10 ℃ min^{-1} for the next 10 min. LA and LNA contents were determined according to the method of Glew et al. (2010). Before analysis, petals were ground to a powder with a mortar and pestle and dried to constant weight under vacuum. Then, 2 g of the sample was extracted using 40 mL of the extraction solution (methanol: chloroform, 1:1, v:v). The extracts were well mixed and filtered. The filtrate was concentrated using a rotary evaporator. Subsequently, at 80°C, the sample was methylated by adding a solution (four drops of benzene, 4 mL of 5% methanol/anhydrous hydrochloric acid), and the LA and LNA contents were assayed using gas chromatography. The following were the gas chromatographic operating settings: (1) H_2 served as the carrier gas, with a flow rate of 1 mL · min^{-1}, (2) the temperatures of the injector and detector were both set at 250 ℃ and (3) the initial temperature was 45 ℃, which was held for 4 min. Then, the temperature was programmed at 13 ℃ · min^{-1} to 175 ℃, which was held for 27 min, and afterward programmed at 4 ℃ · min^{-1} to 215 ℃, which was held for 35 min. ATP content was established by an ATP determination kit (Sigma Chemical Co., St. Louis, USA) in strict conformity with the operational procedures described by the kit. Petal samples (0.5 g) were weighed and added to 5 mL of the lysis buffer from the ATP kit for homogenisation in an ice bath. The homogenate was centrifuged with 8,000 g of petals at 4 ℃ for 10 min. Next, the bioluminescence intensity of the supernatant was determined by a microplate photometer (Multiskan FC, USA). A linear regression equation and serial ATP concentrations were used to determine the ATP content.

Headspace-solid-phase microextraction (HS-SPME)-gas chromatograph and mass spectrometer (GC–MS) analysis

Headspace SPME technology was in time used to extract the samples collected. The volatiles from samples were separated and identified by GC–MS analysis (GC–MS, ThermoFisher Trace ISQ-LT). For HS-SPME to fully extract the volatile components from the samples, the HS bottle was balanced in a water bath at 50 ℃; the microextraction head (Supelco) pre-aged at 250 ℃ for 2 h in the GC injection port was inserted into the HS bottle 1 cm away from the top of the samples for 40 min. The chromatography conditions were as follows: the column was 5% phenyl methyl siloxane (HP-5MS) (0.25 mm × 30 m × 0.25 μm) and carrier gas, helium (99.999%), and column flow rates were 1 mL · min^{-1}. The column temperature was programmed: the initial temperature was maintained at 40 ℃ for 3 min, then ramped to 150 ℃ at 5 ℃ · min^{-1} and then increased to 250 ℃ at 10 ℃ · min^{-1} and held for 5 min. The MS parameters were: ion source temperature 250 ℃; transmission line temperature 250 ℃; ionization voltage 70 eV; mass range m/z 35–450; national institute of standards and technology (NIST) standard reference database number 69. To qualitatively identify floral volatile components, 0.1 μL of n-alkaline mixtures (c6–c20) was used as a standard sample for GC–MS analysis, and their retention indexes (RI) were calculated by a linear heating formula. The relative mass of volatile compounds was calculated by the internal standard method.

Statistical analysis of data

All experimental indicators were evaluated in triplicates, and the measurement data were expressed as the mean plus or minus the standard error (SE). SPSS 17.0 software was used for statistical analysis of the data. One-way analysis of variance (ANOVA) was applied to compare the difference in the mean of the data. Canonical correlation analysis was conducted to explore relationships among the activities of respiratory chain complexes, production rates of precursors and ATP and emissions of floral volatiles.

RESULTS

$ZnSO_4$ treatments increased intracellular Zn^{2+} concentrations

Zn^{2+} fluorescence intensity is an important indicator reflecting the Zn^{2+} concentrations in the cell. ZnAF-2F DA, as a Zn^{2+} fluorescent probe, can be hydrolysed by esterase in the protoplast into ZnAF-2F. The latter can selectively recognise intracellular free Zn^{2+}. When there

was a higher Zn^{2+} concentration in cells, the fluorescence intensity of the complex constituted by the combination of ZnAF-2F and Zn^{2+} was stronger and vice versa. The study indicated that $ZnSO_4$ treatments significantly increased Zn^{2+} fluorescence intensity (Figures 2A–2D, Figures 2a–2d; Table 1). Compared with the control group, the Zn^{2+} fluorescence intensity in 2-8 mM $ZnSO_4$ treatments was stronger (Figures 2A–2D, Figures 2a–2d). Quantitative analysis showed Zn^{2+} fluorescence intensity increased with the increasing $ZnSo_4$ concentration (from 2 mM to 8 mM). In the 8 mM $ZnSo_4$ treatments, both brightfield and darkfield fluorescence intensities reached their maximum values, which were ~54.59% ($p < 0.01$) and ~28.17% ($p < 0.01$), respectively (Table 1). Zn concentrations in petals also showed similar changes (Table 1). In 2–8 mM $ZnSO_4$ treatments, the Zn concentrations were increased by 15.07%, 29.80%, and 81.53%. The results implied that the $ZnSO_4$ application increased the intracellular Zn^{2+} concentrations.

Mitochondrial respiratory chain complex activities were changed by elevated intracellular Zn^{2+} concentrations

To evaluate the response of the activities of mitochondrial respiratory chain complex I, II, III, IV and V to the

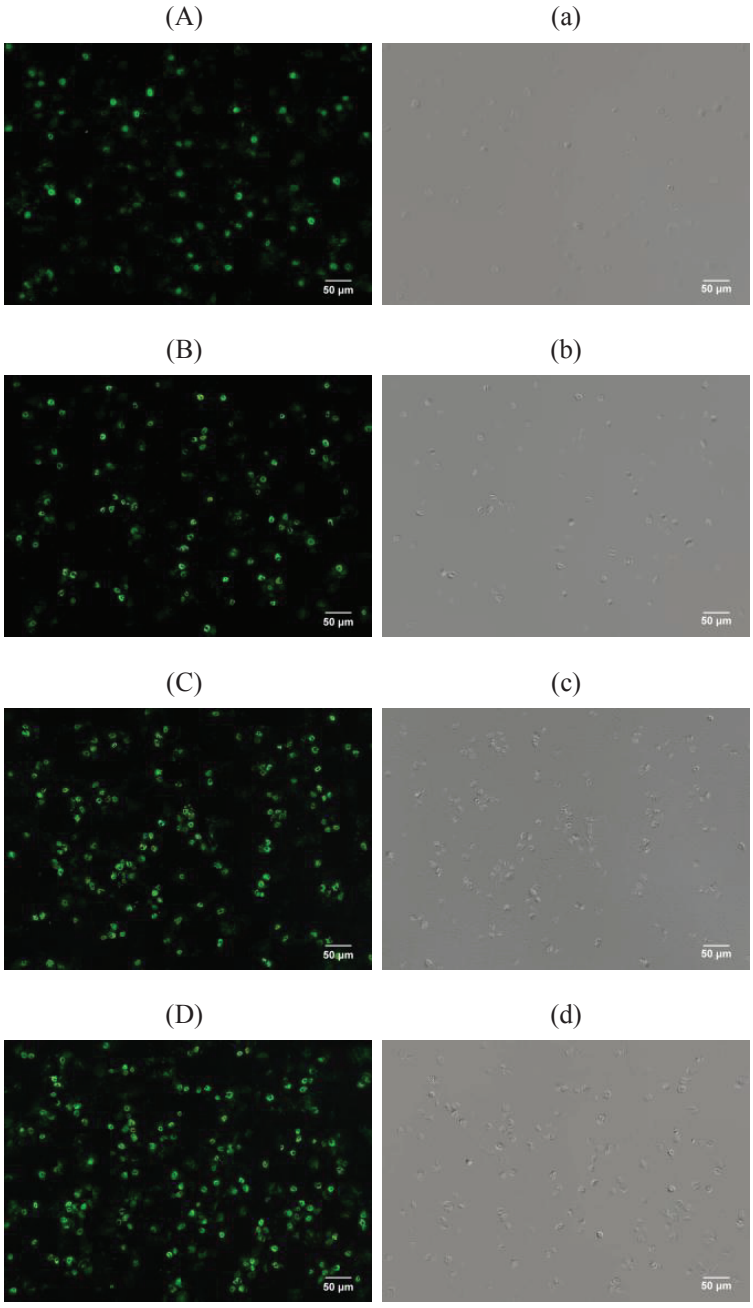

Figure 2. Intracellular Zn^{2+} fluorescence images (A-a, control group; B-b, 2 mM $ZnSO_4$ treatments; C-c, 4 mM $ZnSO_4$ treatments; D-d, 8 mM $ZnSO_4$ treatments) in *D. huoshanense* petals at 6 h after the treatment of different concentrations of $ZnSO_4$. The images were taken in darkfield (A-D) and brightfield (a-d).

Table 1. Zn^{2+} fluorescence intensity and Zn concentrations in *D. huoshanense* petals at 6 h after the treatment of different concentrations of $ZnSO_4$.

$ZnSO_4$ treatments (mM)	Zn^{2+} intensity (mean)		Zn concentrations (mg · kg DM)
	Darkfield	Brightfield	
0	26.56 ± 1.01	93.82 ± 1.35	39.36 ± 2.63
2	27.33 ± 0.80*	99.74 ± 1.52*	45.29 ± 3.85*
4	37.27 ± 1.42**	108.33 ± 0.87**	51.12 ± 3.14**
8	41.06 ± 1.22**	120.25 ± 1.43**	71.45 ± 4.21**

Note: Zn^{2+} intensity is the mean of nine fluorescence measurements. Zinc concentrations are the average value of three measurements. The superscript symbols * and ** indicate that there is a significant difference between means in $p \leq 0.05$ and $p \leq 0.01$, respectively. DM, dry weight.

elevated intracellular Zn^{2+} concentrations, we measured the activity values at 6 h, 9 h and 12 h after the $ZnSO_4$ application (Figures 3A–3E). In 2 mM or 4 mM $ZnSO_4$ treatments, the activity values of complex I, III and IV were not statistically significantly different from those of the control (Figures 3A–3D). However, the activity values of complex II and V were significantly increased, and the increase in activity values varied from 5.42% ($p < 0.05$) to 86.38% ($p < 0.01$) (Figures 3B and 3E). In 8 mM $ZnSO_4$ treatments, the activity values of complex I, II, III, IV and V were all significantly decreased ($p < 0.01$), and the reduction in activity values was at most ~55.39% ($p < 0.01$) (Figures 3A–3E). Elevated intracellular Zn^{2+} concentrations induced the different changes of mitochondrial respiratory chain complex activities.

Precursor and ATP productions were promoted and inhibited by elevated intracellular Zn^{2+} concentrations

Floral volatile emissions can be influenced by precursors and ATP production rates; hence, we measured precursor and ATP contents in *D. huoshanense* petals after the $ZnSO_4$ application (Figures 4A–4F). In 2 mM or 4 mM $ZnSO_4$ treatments, the content of precursors (DMAPP, IPP, Phe, LA and LNA) and ATP was significantly increased with elevated intracellular Zn^{2+} concentrations compared with the control group, and the increase in proportion varied from 3.76% ($p < 0.01$) to 26.15% ($p < 0.01$) and from 21.90% ($p < 0.01$) to 69.43% ($p < 0.01$) in 2 mM and 4 mM $ZnSO_4$ treatments, respectively. However, in 8 mM $ZnSO_4$ treatments, the content of precursors and ATP was significantly decreased, and the decrease in proportion varied from 7.37% ($p < 0.01$) to 27.69% ($p < 0.01$) (Figures 4A–4F). The content changes of precursors and ATP indicated that their production rates in *D. huoshanense* petals were promoted or inhibited by elevated intracellular Zn^{2+} concentrations after $ZnSO_4$ treatments.

Floral volatile emissions were affected by elevated intracellular Zn^{2+} concentrations

The total ion chromatograms of volatile components were obtained by GC–MS analysis, including the different concentrations of $ZnSO_4$-treated samples at 6 h, 9 h and 12 h (Figures S1A–S1D, Figures S2A–S2D, Figures S3A–S3D). Based on the retrieved data of the MS library, floral volatile components were distinguished and are listed in Table 2. A total of 42 volatile compounds, with a total mass of 59.01 $\mu g \cdot g^{-1}$ FW, were identified in the control group, including 17 terpenoids, 38.38 $\mu g \cdot g^{-1}$ FW; 5 benzoids, 2.53 $\mu g \cdot g^{-1}$ FW; and 21 fatty acid derivatives, 18.10 $\mu g \cdot g^{-1}$ FW. Compared with the control group, 2 mM and 4 mM $\cdot L^{-1}$ $ZnSO_4$ treatments promoted floral violate emissions; the number of floral volatile compounds increased by one (2 mM $ZnSO_4$ treatments) and three (4 mM $ZnSO_4$ treatments), and their total mass increased by 18.09% ($p < 0.01$), 66.88% ($p < 0.01$) respectively; in addition, the mass of terpenoids, benzoids and fatty acid derivatives all increased. However, 8 mM $ZnSO_4$ treatments significantly reduced floral violate emissions; there were only 39 compounds, losing 3 compounds compared with the control group; the total mass of volatile compounds decreased by 18.79% ($p < 0.01$), and the mass of terpenoids, benzoids and fatty acid derivatives all decreased (Figures 5A–5D; Table 2). The mass and number changes of floral volatile compounds indicated that their emissions in *D. huoshanense* petals were affected by elevated intracellular Zn^{2+} concentrations after $ZnSO_4$ treatments.

Canonical correlation analysis between activities of mitochondrial respiratory chain complexes or emissions of floral volatiles and productions of precursors and ATP

Canonical correlation analysis is a statistical method for studying the overall relevance between two sets of variables, which can more comprehensively reflect the internal relationship between variable sets. Thus, we performed canonical correlation analysis to understand the overall relationships among the activities of mitochondrial respiratory chain complexes (X group), productions of precursors and ATP (Y group) and emissions of floral volatiles (Z group) (Figures 6A–6C, Tables S1–S3). The diagram in Figure 6A shows that the canonical coefficient of this pair of variables (X group, Y group) is 0.999 and statistically significant at the 1% level, indicating that there is a very close positive correlation between the five indicators in the X group

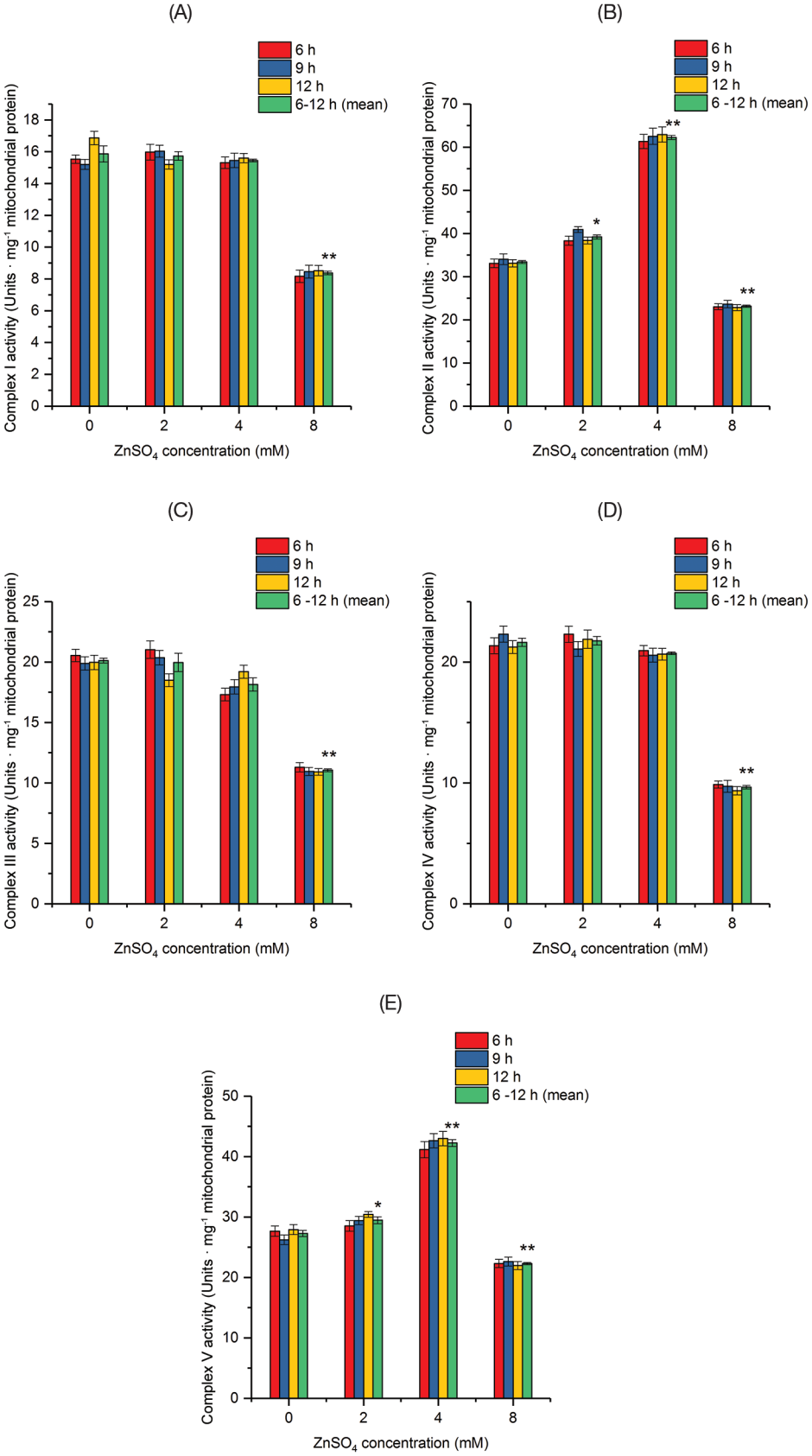

Figure 3. Effects of different concentrations of $ZnSO_4$ at different times on treatments since the treatment on average ± SE activities of mitochondrial respiratory chain complex I (A), II (B), III (C), IV (D) and V (E) in *D. huoshanense* petals. The superscript symbols * and ** indicate that there is a significant difference between means in $p \leq 0.05$ and $p \leq 0.01$, respectively. SE, standard error.

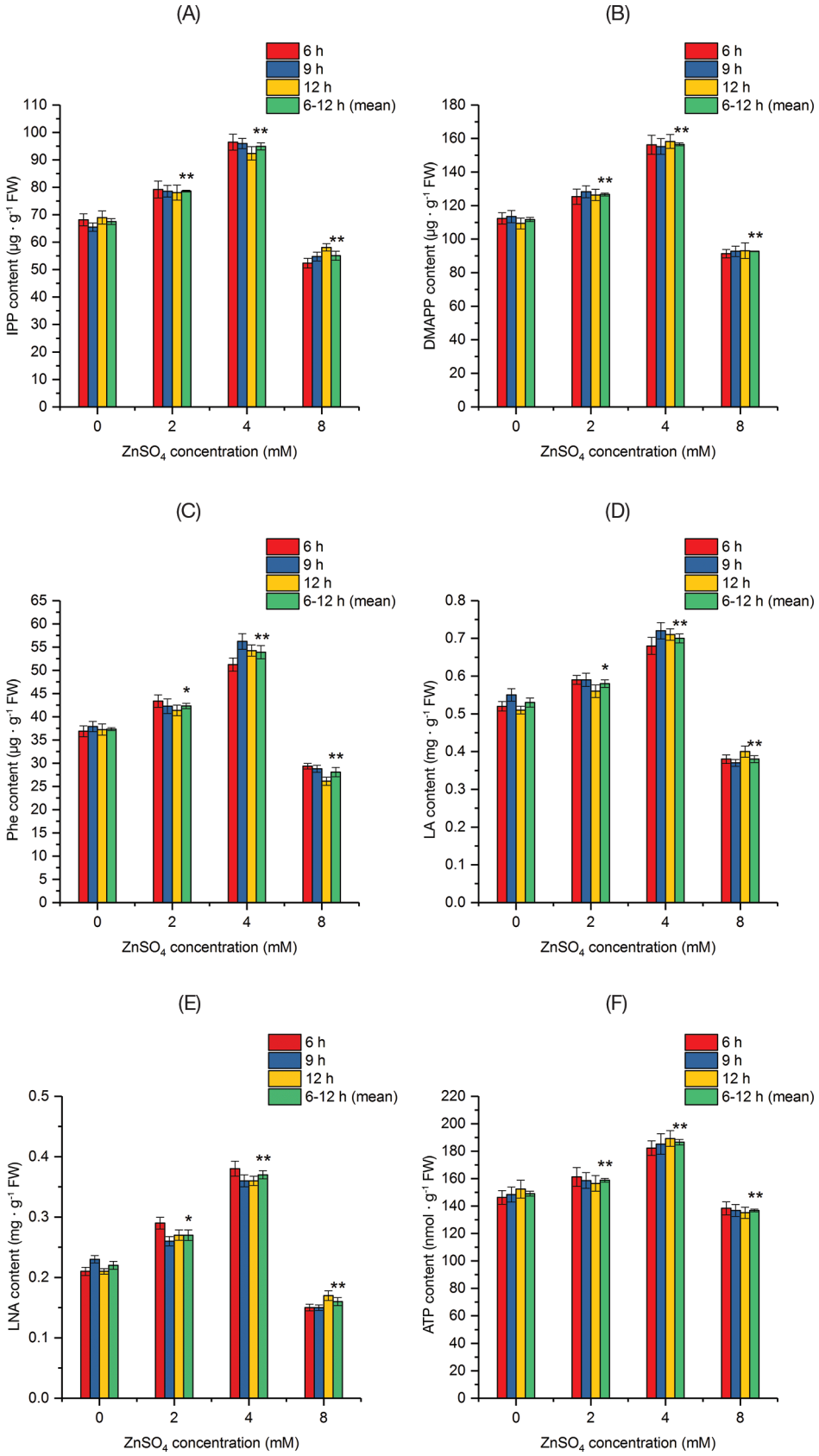

Figure 4. Effects of $ZnSO_4$ treatments on precursor (IPP, A; DMAPP, B; Phe, C; LA, D; LNA, E) and ATP (F) levels in *D. huoshanense* petals. The superscript symbols * and ** indicate that there is a significant difference between means in $p \leq 0.05$ and $p \leq 0.01$, respectively. IPP, isopentenyl pyrophosphate; DMAPP, dimethylallyl pyrophosphate; Phe, phenylalanine, LA, linoleic acid; LNA, linolenic acid, ATP, adenosine triphosphate.

Table 2. Component of floral volatiles from *D. huoshanense* petals treated with different concentrations of $ZnSO_4$. The values of component contents ± SE in Table 2 were an average of their contents at 6 h, 9 h and 12 h after $ZnSO_4$ treatments.

Component code	Component name	RI (retention time) calculation value	RI (retention time) reference value	Component content (μg · g^{-1} FW)			
				$ZnSO_4$ concentrations (mM)			
				0	2	4	8
Monoterpenes (C 10) and sesquiterpenes (C 15) and terpenoid derivatives							
A1	α-Pinene	936	939	0.82 ± 0.01	0.76 ± 0.02	0.85 ± 0.03	0.72 ± 0.03
A2	1,8-Cineol	1,018	1,015	0.34 ± 0.01	0.34 ± 0.02	0.39 ± 0.02	0.32 ± 0.02
A3	α-Ocimene	1,023	1,018	0.65 ± 0.03	0.67 ± 0.01	0.75 ± 0.02	0.83 ± 0.02
A4	β-Ocimene	1,049	1,044	16.49 ± 0.13	17.56 ± 0.15	19.62 ± 0.14	13.97 ± 0.11
A5	β-trans-Ocimene	1,056	1,050	1.45 ± 0.03	4.93 ± 0.06	2.02 ± 0.03	0.61 ± 0.01
A6	α-Cyclocitral	1,091	1,102	0.32 ± 0.02	0.28±0.03	0.26 ± 0.02	0.41 ± 0.03
A7	Linalool	1,096	1,102	0.66 ± 0.02	0.69 ± 0.02	0.63 ± 0.02	0.68 ± 0.01
A8	(E,E)-2,6-Dimethyl-2,4,6-octatriene	1,135	1,143.5	-	-	0.68 ± 0.03	-
A9	(E)-Isopentyl 2-methylbut-2-enoate	1,189	1,195.8	0.75 ± 0.01	0.75 ± 0.02	0.85 ± 0.02	1.09 ± 0.02
A10	β-Cyclocitral	1,218	1,214	0.16 ± 0.03	0.16 ± 0.01	0.17 ± 0.01	-
A11	Geraniol	1,258	1,254	0.65 ± 0.02	0.83 ± 0.01	1.06 ± 0.02	3.04 ± 0.03
A12	δ-Elemene	1,321	1,324	0.91 ± 0.03	2.09 ± 0.04	5.38 ± 0.05	1.14 ± 0.10
A13	β-Elemene	1,369	1,373	0.46 ± 0.02	0.47 ± 0.01	0.42 ± 0.02	0.48 ± 0.03
A14	α-Ionone	1,421	1,426	0.38 ± 0.03	2.84 ± 0.03	0.43 ± 0.02	0.40 ± 0.02
A15	β-Caryophillene	1,425	1,417	10.46 ± 0.08	7.54 ± 0.06	20.73 ± 0.06	4.60 ± 0.05
A16	α,β-Dihydro-b-ionone	1,438	1,433	2.13 ± 0.04	1.38 ± 0.04	1.83 ± 0.03	0.96 ± 0.02
A17	Geranyl acetone	1,459	1,455	1.32 ± 0.02	1.79 ± 0.03	2.56 ± 0.06	0.92 ± 0.02
A18	α-Farnesene	1,516	1,507	3.13 ± 0.06	8.05 ± 0.09	6.12 ± 0.05	1.48 ± 0.04
A19	α-Cedrene epoxide	1,598	1,570	0.29 ± 0.03	0.30 ± 0.03	0.33 ± 0.01	0.27 ± 0.01
A20	Caryophyllene oxide	1,623	1,593	0.46 ± 0.05	0.45 ± 0.05	0.50 ± 0.03	0.36 ± 0.02
A21	(E, E) -Farnesol	1,692	1,722	0.38 ± 0.01	0.34 ± 0.03	0.39 ± 0.02	0.24 ± 0.02
Benzoids							
B1	1-Ethenyl-4-methoxybenzene	1,149	1,151.6	1.02 ± 0.01	1.14 ± 0.02	1.46 ± 0.21	0.84 ± 0.01
B2	1,4-Dimethoxybenzene	1,158	1,165	0.82 ± 0.02	0.86 ± 0.02	0.97 ± 0.02	0.74 ± 0.01
B3	4-(2-Propenyl) phenol	1,249	1,254	0.14 ± 0.01	0.14 ± 0.02	0.16 ± 0.02	-
B4	1,3-Dimethoxy-5-methylbenzene	1,263	1,260	0. 22 ± 0. 01	0. 22 ± 0. 02	0. 19 ± 0. 02	0. 26 ± 0. 02
B5	3-methoxy-5-methylphenol	1,340	1,342	0. 33 ± 0. 02	0. 33 ± 0. 03	0. 32 ± 0. 01	0. 33 ± 0. 02
B6	Butylated Hydroxytoluene	1,507	1,511	-	-	1.65 ± 0.02	-
Fatty acid derivatives							
C1	3-Methylbutanoic acid methyl ester	769	765	0.46 ± 0.02	0.63 ± 0.05	0.81 ± 0.03	0.22 ± 0.02
C2	2-Methylbutyric acid, methyl ester	778	780	0.27 ± 0.03	0.25 ± 0.02	0.25 ± 0.01	0.25 ± 0.03
C3	Hexanal	793	800	0.21 ± 0.01	0.18 ± 0.03	0.24 ± 0.02	0.20 ± 0.02
C4	2-Hexanol	806	803	0.85 ± 0.02	0.97 ± 0.01	1.57 ± 0.04	0.64 ± 0.02
C5	Acetic acid, butyl ester	809	812	0.59 ± 0.03	0.54 ± 0.02	0.66 ± 0.04	0.53 ± 0.02
C6	2-Methylbutanoic acid ethyl ester	841	846	0.56 ± 0.01	0.59 ± 0.021	0.68 ± 0.03	-
C7	(Z)-Hex-3-en-1-ol	849	851	0.45 ± 0.03	0.29 ± 0.02	0.51 ± 0.02	0.39 ± 0.03
C8	1-Hexanol	856	867	1.41 ± 0.04	1.04 ± 0.02	6.33 ± 0.08	3.02 ± 0.01
C9	3-Methylbutanoic acid ethyl ester	857	859	0.32 ± 0.02	1.11 ± 0.03	1.65 ± 0.04	0.51 ± 0.01

(*Continued*)

Table 2. Continued.

Component code	Component name	RI (retention time) calculation value	RI (retention time) reference value	Component content (μg · g^{-1} FW)			
				$ZnSO_4$ concentrations (mM)			
				0	2	4	8
C10	Acetic acid, 3-methylbutyl ester	881	876	0.47 ± 0.03	0.37 ± 0.01	0.42 ± 0.01	0.40 ± 0.02
C11	Tiglic acid ethyl ester	952	949	-	1.28 ± 0.05	1.74 ± 0.02	-
C12	1-Heptanol	975	970	1.08 ± 0.04	2.56 ± 0.06	1.56 ± 0.02	0.89 ± 0.02
C13	1-Octen-3-ol	998	986	0.94 ± 0.02	1.16 ± 0.01	1.78 ± 0.01	0.73 ± 0.02
C14	3-Octanone	1,003	987	4.53 ± 0.09	1.78 ± 0.02	7.33 ± 0.03	2.84 ± 0.03
C15	3-Octanol	1,009	995	0.51 ± 0.01	0.47 ± 0.02	0.54 ± 0.02	0.49 ± 0.01
C16	(E) -2-Octen-1-ol	1,062	1,067	0.51 ± 0.01	0.52 ± 0.01	0.58 ± 0.02	0.99 ± 0.02
C17	Nonanal	1,110	1,089	0.44 ± 0.02	0.35 ± 0.02	0.33 ± 0.02	0.48 ± 0.01
C18	3-Nonen-2-one	1,142	1,136	0.67 ± 0.02	0.69 ± 0.03	0.78 ± 0.03	0.65 ± 0.02

Notes: "-" means not detected.

RI, retention indexes; SE, standard error; FW, fresh weight.

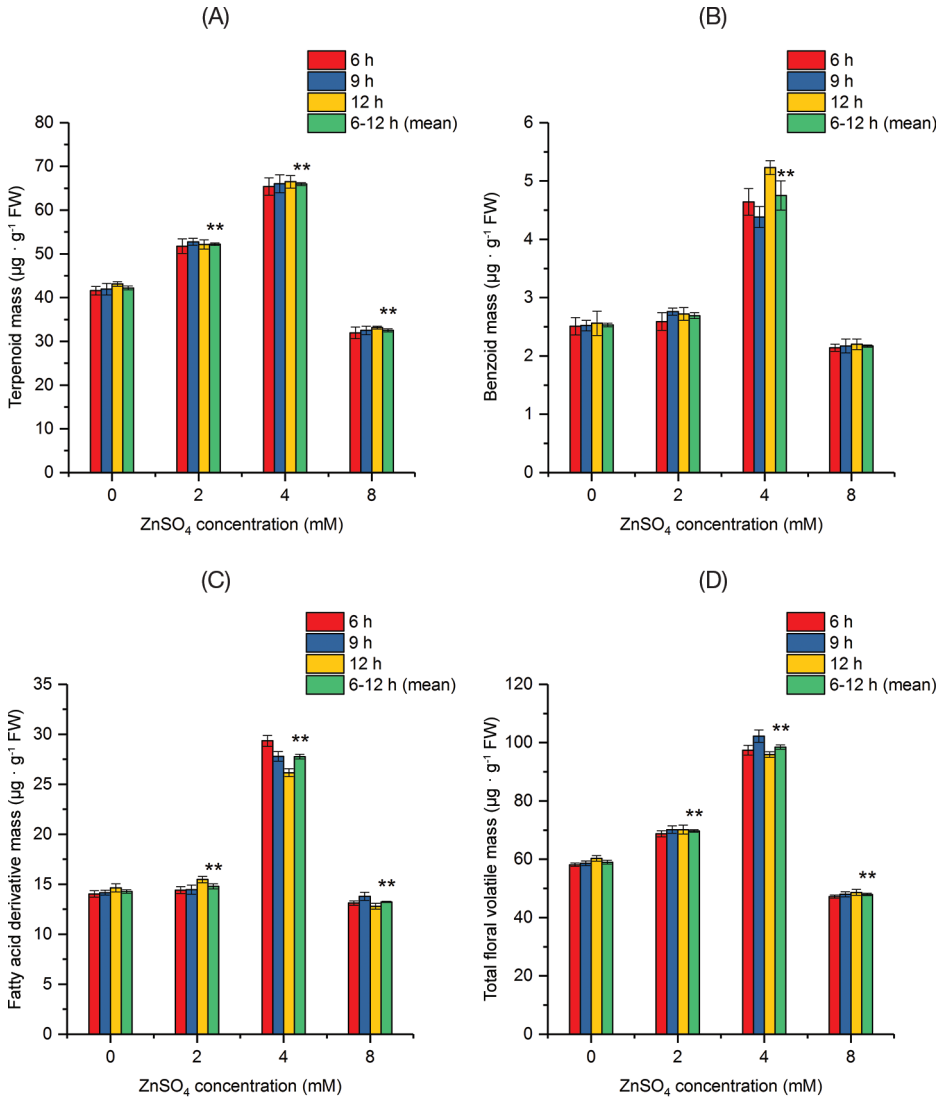

Figure 5. Effects of $ZnSO_4$ treatments on emissions of terpenoids (A), benzenes (B), fatty acid derivatives (C) and total floral volatiles (D) from *D. huoshanense* petals. The superscript symbols * and ** indicate that there is a significant difference between means in $p \leq 0.05$ and $p \leq 0.01$, respectively.

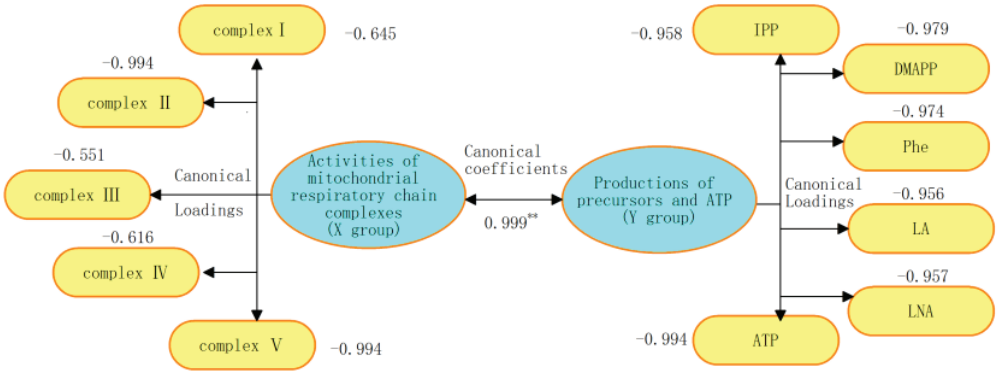

(A)

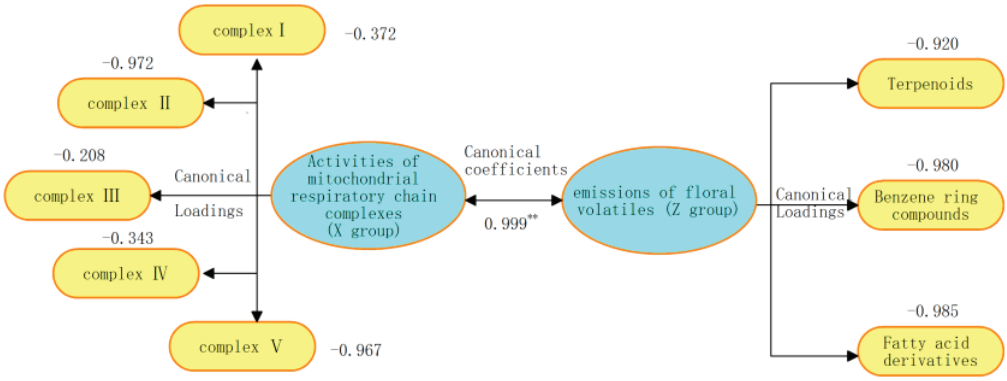

(B)

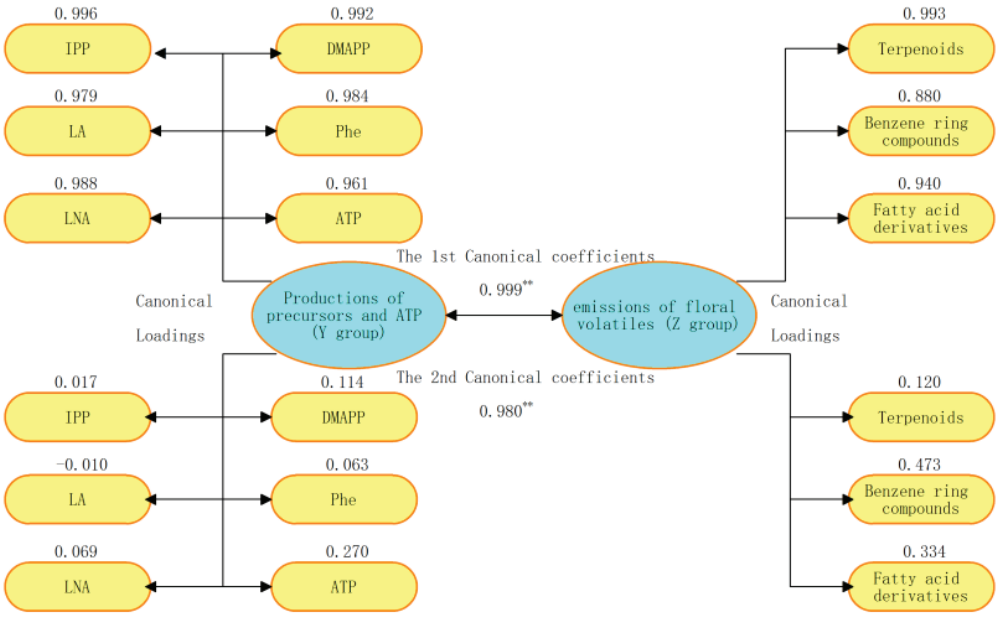

(C)

Figure 6. Structure diagram of canonical correlation analysis among the activities of mitochondrial respiratory chain complexes (X group), production rates of precursors and ATP (Y group) and emissions of floral volatiles (Z group). (A) shows there is a significantly positive correlation between the X group and the Y group at the statistical 1% level. Similar to (A), (B) also shows a statistical correlation between the X and Z groups. (C) has two canonical correlation coefficients, and they are both statistically significant at the 1% level, indicating that there is a very close positive correlation between the Y and Z group even though their internal canonical loading of each indicator inside the Y and Z group is different. The superscript symbols * and ** indicate that there is a significant difference in the correlation coefficients between the X group, the Y group and the Z group in $p \leq 0.05$ and $p \leq 0.01$, respectively. ATP, adenosine triphosphate, Phe, phenylalanine; IPP, isopentenyl pyrophosphate; LA, linoleic acid; LNA, linolenic acid; DMAPP, dimethylallyl pyrophosphate.

and the six indicators in the Y group. By analysing the internal structure of the X or Y group, it is found that a canonical load of complex II and V is relatively larger in the X group and a canonical load of ATP in the Y group too. Similar to Figure 6A, Figure 6B shows there are also positive correlations between X and Z groups. The diagram in Figure 6C shows that there are two canonical coefficients between the Y and Z group, and the two canonical coefficients are both statistically significant at the 1% level, indicating that there is a very close positive correlation between the six indicators in the Y group and the three indicators in the Z group. In the internal structure of the Y and Z group, the canonical load of each indicator affiliated to the first correlation coefficient is larger than corresponding to that affiliated to the second correlation coefficient. In conclusion, canonical correlation analysis of the above variable sets indicates that there are overall positive relations among mitochondrial respiratory chain complex activities, precursor and ATP productions and floral volatile emissions.

DISCUSSION

Elevated intracellular Zn^{2+} concentrations changed activities of mitochondrial respiratory chain complexes

In the present study, intracellular Zn^{2+} concentrations treated with 2 mM, 4 mM and 8 mM exogenous Zn^{2+} are all increased significantly (Figures 2A–2D, Figures 2a–2d, Table 1). This indicates that the exogenous Zn^{2+} treatments have obvious effects on intracellular Zn^{2+} regulation in *D. huoshanense*. Under normal physiological conditions, the total Zn^{2+} level in plant cells is strictly regulated (Colvin et al., 2010). When cells are stimulated by a low concentration of Zn^{2+}, intracellular Zn^{2+} concentrations can remain relatively stable because the intracellular Zn^{2+} concentration can be regulated by a cell wall barrier, absorption, and the mechanism of Zn^{2+} transfer into and out of cells. But when cells are stimulated by a high concentration of Zn^{2+}, the Zn^{2+} concentration inside the cells may increase due to exceeding the self-regulating ability of intracellular Zn^{2+} (Eide, 2006; Colvin et al., 2010). Given exogenous Zn^{2+} treatments in this study exceeded the self-regulation ability of the cells, the intracellular Zn^{2+} concentrations were increased in petal cells of *D. huoshanense*. The elevated concentration of Zn^{2+} may be an intracellular signal to induce or directly participate in the regulation of physiological and biochemical activity in cells by complex-mediated pathways, affect enzyme activities and change material and energy metabolism. For example, Amiri et al. (2015) reported that a high concentration of exogenous Zn^{2+} treatment significantly increased the activity of superoxide dismutase in almond seedlings under salt stress.

Further, this study showed that elevated intracellular Zn^{2+} concentrations had diverse effects on the activities of mitochondrial respiratory chain complex I, II, III, IV and V (Figures 3A–3E). This may be attributed to the fact that Zn^{2+} can regulate protease activity in various ways. Zn^{2+} has a strong ability to accept electrons and can combine with some nitrogen, sulphur and other atoms in proteins through electrostatic attraction to form a tetrahedral structure that plays an important role in protease function display (Takahashi et al., 2003). Zn^{2+} can also act as an activator and regulator of some enzymes (Rezaeieh et al., 2016). Many studies have shown that there are one or more zinc-binding sites in respiratory chain complex I, III, IV and V (Sharpley and Hirst et al., 2006; Vygodina et al., 2008; Rose et al., 2011; Yi et al., 2017); due to differences in the zinc-binding rate and plasticity at discrete sites, their activities are variable under different Zn^{2+} concentration treatments. For complex II, although there are limited reports about the influence of Zn^{2+} as a structural function on its activity, Zn^{2+} can exert an effect through the activation and regulation function (Pan et al., 2013). All in all, intracellular Zn^{2+}, in theory, can act on respiratory chain complexes (I, II, III, IV and V) through structural, activating or regulatory functions. Different Zn^{2+} concentrations have various effects on the activity of respiratory chain complexes because of the difference in the action mechanism of Zn^{2+} on respiratory chain complexes.

Changes in activities of mitochondrial respiratory chain complexes affect floral volatile emissions

Mitochondria are semi-autonomous organelle. The signalling of mitochondrial to nucleus is termed as retrograde signalling, which can participate in the regulation of cellular material and energy metabolism (Carlsson et al., 2008). Studies have shown that mitochondrial alternative oxidase pathways can affect plant volatile emissions (Chen et al., 2020). But, so far, there are limited reports on the relationship between the activities of mitochondrial respiratory chain complexes and floral volatile emissions.

In theory, respiratory chain complex II is directly involved in the TCA cycle, while complex I, III, IV and V indirectly affect the TCA cycle and directly affect oxidative phosphorylation by electron transfer (Pan et al., 2013; Heidarvand et al., 2017). Changes in the mitochondrial respiratory chain and the TCA cycle can induce nuclear genes to regulate metabolic intermediate and ATP productions (Carlsson et al., 2008). Our research results directly confirmed that changes in the activity of respiratory chain complexes affected precursor and ATP productions in *D. huoshanense*. For example, in the 2 mM or 4 mM $ZnSO_4$ treatments, the activities of respiratory chain complex II and V significantly enhanced (Figures 3B and 3E), and the precursor and ATP productions increased (Figures 4A–4F). Canonical correlation analysis further confirmed that changes in respiratory chain complex activities were significantly

correlated with the production of precursors and ATP. Moreover, within the respiratory chain complexes, complex II and V have relatively larger canonical loadings, indicating that they are the main factors causing changes in the production of precursors and ATP (Figure 6A). Other studies also have shown that complex II and V are closely linked to the TCA cycle, oxidative phosphorylation and production of precursors and ATP (Pan et al., 2013; Lee and Chen, 2014; Liang et al., 2019).

Floral volatile emissions are regulated by a precursor and ATP supply. Firstly, flower volatiles are mainly synthesised by the mevalonic acid (MEP)/the methylerythritol-phosphate (MVA) pathway, shikimic acid (SKA) pathway and LOX pathway (Gentner et al., 2014). In the MEP/MVA pathway, terpenoids are regulated by the supply of IPP and DMAPP; in the SKA pathway, benzoids are regulated by the supply of Phe; while in the SKA pathway, fatty acid derivatives are regulated by the supply of LA and LNA (van Schie et al., 2006; Gentner et al., 2014). Secondly, the emissions of floral volatiles require energy. It was reported that floral volatiles are synthesised in plant sub-organelles; their emission must at least cross the barrier of the cytosol, plasma membrane, hydrophilic cell wall and sometimes the cuticle (Adebesin et al., 2017). This was also confirmed by our study. After being treated with different concentrations of Zn^{2+}, floral volatile emissions correspondingly increased or decreased with up or down of the precursor and ATP levels, and there is a significant positive correlation between the former and the latter (Figures 4A–4F, Figures 5A–5D, Figure 6C). Therefore, when the level of IPP and DMAPP was higher, the category and quantity of terpenoids are more. Similarly, the relationship between Phe and benzoids or between LA and LNA and fatty acid derivatives is similar. As for ATP, it provides energy for their emissions.

In summary, our research results confirmed that changes in the activity of respiratory chain complexes, especially complex II and V, affected volatile emissions by regulating precursor and ATP productions in *D. huoshanense*. However, it remains still unclear how the changes in mitochondrial complex activities trigger the mitochondrial-to-nucleus gene retrograde signalling to regulate precursor and ATP productions, as well as floral violate emissions. Further study needs to be focussed on this point.

CONCLUSIONS

In this study, we demonstrated the relation between Zn^{2+} concentrations and floral volatile emissions in *D. huoshanense*. Further, we demonstrated that there are significant positive correlations between mitochondrial respiratory chain complex activities and floral volatile emissions. Particularly, changes mainly in complex II and V activities increased or inhibited precursor (IPP and DMAPP, Phe and LA and LNA) and ATP productions, leading to corresponding changes in floral volatile emissions of terpenoids, benzoids and fatty acid derivatives. Our results will contribute to understanding the relationship between Zn^{2+} and floral volatile emissions from the perspective of mitochondrial function. In future studies, the mechanism of mitochondrial complex activities that trigger the mitochondrial-to-nucleus gene retrograde signalling to regulate flower violate emissions should be further investigated.

FUNDING

This research was supported by the National Natural Science Foundation of China (81573536) and the Key Project of the Natural Science of Universities of Anhui Province (KJ2018A0421, KJ2019A0628, KJ2016A747, WGKQ2021030).

AUTHOR CONTRIBUTIONS

W.Z. and J.W. designed the experiments and wrote the manuscript. W.Z., J.W. and J.D. performed the experiments. W.Z. and J.D. analysed and counted the data. All authors read and approved the final manuscript.

CONFLICT OF INTEREST

No conflict of interest exists in the submission of this manuscript.

REFERENCES

Abbas, F., Ke, Y., Yu, R., and Fan, Y. (2019). Functional characterization and expression analysis of two terpene synthases involved in floral scent formation in *Lilium* 'Siberia'. *Planta, 249*(1), 71–93, doi: 10.1007/s00425-018-3006-7.

Adebesin, F., Widhalm, J. R., Boachon, B., Lefèvre, F., Pierman, B., Lynch, J. H., and Dudareva, N. (2017). Emission of volatile organic compounds from petunia flowers is facilitated by an ABC transporter. *Science, 356*(6345), 1386–1388, doi: 10.1126/science.aan0826.

Amiri, A., Baninasab, B., Ghobadi, C., and Khoshgoftarmanesh, A. H. (2015). Zinc soil application enhances photosynthetic capacity and antioxidant enzyme activities in almond seedlings affected by salinity stress. *Photosynthetica, 54*(2), 267–274, doi: 10.1007/s11099-016-0078-0.

Ashok Kumar, A., Reddy, B. V. S., Ramaiah, B., Sahrawat, K. L., and Pfeiffer, W. H. (2013). Gene effects and heterosis for grain iron and zinc concentration in sorghum [*Sorghum bicolor* (L.) Moench]. *Field Crops Research, 146*, 86–95, doi: 10.1016/j.fcr.2013.03.001.

Barman, M., and Mitra, A. (2019). Temporal relationship between emitted and endogenous floral scent volatiles in summer- and winter-blooming *Jasminum* species. *Physiologia Plantarum, 166*(4), 946–959, doi: 10.1111/ppl.12849.

Bautista-Diaz, J., Cruz-Alvarez, O., Hernández-Rodríguez, O. A., Sánchez-Chávez, E., Jacobo-Cuellar, J. L., Preciado-Rangel, P., and Ojeda-Barrios, D. L. (2021). Zinc sulphate or zinc nanoparticle applications to leaves of green beans. *Folia Horticulturae, 33*(2), 365–375, doi: 10.2478/fhort-2021-0028.

Bera, P., Mukherjee, C., and Mitra, A. (2017). Enzymatic production and emission of floral scent volatiles in *Jasminum sambac*. *Plant Science, 256*, 25–38, doi: 10.1016/j.plantsci.2016.11.013.

Campbell, D. R., Sosenski, P., and Raguso, R. A. (2019). Phenotypic plasticity of floral volatiles in response to increasing drought stress. *Annals of Botany, 123*(4), 601–610, doi: 10.1093/aob/mcy193.

Carlsson, J., Leino, M., Sohlberg, J., Sundstrom, J. F., and Glimelius, K. (2008). Mitochondrial regulation of flower development. *Mitochondrion, 8*(1), 74–86, doi: 10.1016/j.mito.2007.09.006.

Chen, S., Dai, J., Song, X., Jiang, X., Zhao, Q., Sun, C., and Han, B. (2020). Endophytic microbiota comparison of *Dendrobium huoshanense* root and stem in different growth years. *Planta Medica, 86*(13–14), 967–975, doi: 10.1055/a-1046-1022.

Chuang, Y. C., Lee, M. C., Chang, Y. L., Chen, W. H., and Chen, H. H. (2017). Diurnal regulation of the floral scent emission by light and circadian rhythm in the *Phalaenopsis* orchids. *Botanical Studies, 58*(1), 50, doi: 10.1186/s40529-017-0204-8.

Cogliati, S., Lorenzi, I., Rigoni, G., Caicci, F., and Soriano, M. E. (2018). Regulation of mitochondrial electron transport chain assembly. *Journal of Molecular Biology, 430*(24), 4849–4873, doi: 10.1016/j.jmb.2018.09.016.

Colvin, R. A., Holmes, W. R., Fontaine, C. P., and Maret, W. (2010). Cytosolic zinc buffering and muffling: Their role in intracellular zinc homeostasis. *Metallomics, 2*(5), 306–317, doi: 10.1039/b926662c.

Cordeiro, G. D., Fernandes Dos Santos, I. G., Silva, C. I. D., Schlindwein, C., Alves-Dos-Santos, I., and Dotterl, S. (2019). Nocturnal floral scent profiles of Myrtaceae fruit crops. *Phytochemistry, 162*, 193–198, doi: 10.1016/j.phytochem.2019.03.011.

Eide, D. J. (2006). Zinc transporters and the cellular trafficking of zinc. *Biochim Biophys Acta, 1763*(7), 711–722, doi: 10.1016/j.bbamcr.2006.03.005.

Estornell, E., Fato, R., Pallotti, F., and Lenaz, G. (1993). Assay conditions for the mitochondrial NADH:coenzyme Q oxidoreductase. *FEBS Lett, 332*(1–2), 127–131, doi: 10.1016/0014-5793(93)80498-j.

Farooq, M., Ullah, A., Rehman, A., Nawaz, A., Nadeem, A., Wakeel, A., and Siddique, K. H. M. (2018). Application of zinc improves the productivity and biofortification of fine grain aromatic rice grown in dry seeded and puddled transplanted production systems. *Field Crops Research, 216*, 53–62, doi: 10.1016/j.fcr.2017.11.004.

Fedor, J. G., and Hirst, J. (2018). Mitochondrial supercomplexes do not enhance catalysis by quinone channeling. *Cell Metabolism, 28*(3), 525–531, e524, doi: 10.1016/j.cmet.2018.05.024.

Fu, J., Hou, D., Zhang, C., Bao, Z., Zhao, H., and Hu, S. (2017). The emission of the floral scent of four *Osmanthus fragrans* cultivars in response to different temperatures. *Molecules, 22*(3), 430, doi: 10.3390/molecules22030430.

Gentner, D. R., Ormeño, E., Fares, S., Ford, T. B., Weber, R., Park, J. H., and Goldstein, A. H. (2014). Emissions of terpenoids, benzenoids, and other biogenic gas-phase organic compounds from agricultural crops and their potential implications for air quality. *Atmospheric Chemistry and Physics, 14*(11), 5393–5413, doi: 10.5194/acp-14-5393-2014.

Glew, R. H., Kramer, J. K. G., Ernst, J., Hernandez, M., N., N. D., Pastuszyn, A., and VanderJagt, D. J. (2010). The amino acid, mineral and fatty acid content of three species of human plant foods in Cameroun. *Food, 4*(1), 1–6.

Guilley, E., and Hahne, G. (1989). Callus formation from isolated sunflower (*Helianthus annuus*) mesophyll protoplasts. *Plant Cell Reports, 8*(4), 226–229, doi: 10.1007/BF00778539.

Han, Y., Wang, H., Wang, X., Li, K., Dong, M., Li, Y., and Shang, F. (2019). Mechanism of floral scent production in *Osmanthus fragrans* and the production and regulation of its key floral constituents, beta-ionone and linalool. *Horticulture Research, 6*, 106, doi: 10.1038/s41438-019-0189-4.

Heidarvand, L., Millar, A. H., and Taylor, N. L. (2017). Responses of the mitochondrial respiratory system to low temperature in plants. *Critical Reviews in Plant Sciences, 36*(4), 217–240, doi: 10.1080/07352689.2017.1375836.

Hu, Z., Li, T., Zheng, J., Yang, K., He, X., and Leng, P. (2015). Ca^{2+} signal contributing to the synthesis and emission of monoterpenes regulated by light intensity in *Lilium* 'siberia'. *Plant Physiology and Biochemistry, 91*, 1–9, doi: 10.1016/j.plaphy.2015.03.005.

Huang, M., Fan, R., Ye, X., Lin, R., Luo, Y., Fang, N., and Chen, S. (2018). The transcriptome of flower development provides insight into floral scent formation in Freesia hybrida. *Plant Growth Regulation, 86*(1), 93–104, doi: 10.1007/s10725-018-0413-5.

Jin, Q., Jiao, C., Sun, S., Song, C., Cai, Y., Lin, Y., and Zhu, Y. (2016). Metabolic analysis of medicinal *Dendrobium officinale* and *Dendrobium huoshanense* during different growth years. *PLoS ONE, 11*(1), e0146607, doi: 10.1371/journal.pone.0146607.

Lee, P.-L., and Chen, J.-T. (2014). Plant regeneration via callus culture and subsequent in vitro flowering of *Dendrobium huoshanense*. *Acta Physiologiae Plantarum, 36*(10), 2619–2625, doi: 10.1007/s11738-014-1632-7.

Li, M., Guo, R., Jiao, Y., Jin, X., Zhang, H., and Shi, L. (2017). Comparison of salt tolerance in soja based on metabolomics of seedling roots. *Frontiers in Plant Science, 8*, 1101, doi: 10.3389/fpls.2017.01101.

Liang, Z. Y., Zhang, J. Y., Huang, Y. C., Zhou, C. J., Wang, Y. W., Zhou, C. H., and Wei, G. (2019). Identification of flavonoids in *Dendrobium huoshanense* and comparison with those in allied species of *Dendrobium* by TLC, HPLC and HPLC coupled with electrospray ionization multi-stage tandem MS analyses. *Journal of Separation Science, 42*(5), 1088–1104, doi: 10.1002/jssc.201801021.

Mohd-Hairul, A. R., Namasivayam, P., Cheng Lian, G. E., and Abdullah, J. O. (2010). Terpenoid, benzenoid, and phenylpropanoid compounds in the floral scent of *Vanda* Mimi Palmer. *Journal of Plant Biology, 53*(5), 358–366, doi: 10.1007/s12374-010-9123-x.

Muhlemann, J. K., Klempien, A., and Dudareva, N. (2014). Floral volatiles: from biosynthesis to function. *Plant, Cell & Environment, 37*(8), 1936–1949, doi: 10.1111/pce.12314.

Olechnowicz, J., Tinkov, A., Skalny, A., and Suliburska, J. (2018). Zinc status is associated with inflammation, oxidative stress, lipid, and glucose metabolism. *The Journal of Physiological Sciences, 68*(1), 19–31, doi: 10.1007/s12576-017-0571-7.

Pan, L.-H., Feng, B.-J., Wang, J.-H., Zha, X.-Q., and Luo, J.-P. (2013). Structural characterization and anti-glycation activityin vitroof a water-soluble polysaccharide from *Dendrobium huoshanense*. *Journal of Food Biochemistry, 37*(3), 313–321, doi: 10.1111/j.1745-4514.2011.00633.x.

Petrussa, E., Bertolini, A., Krajnakova, J., Casolo, V., Macri, F., and Vianello, A. (2008). Isolation of mitochondria from embryogenic cultures of *Picea abies* (L.) Karst. and *Abies cephalonica* Loud.: characterization of a K^+_{ATP} channel. *Plant Cell Reports, 27*(1), 137–146, doi: 10.1007/s00299-007-0436-2.

Qi, W., Wang, H., Zhou, Z., Yang, P., Wu, W., Li, Z., and Li, X. (2020). Ethylene emission as a potential indicator of Fuji apple flavor quality evaluation under low temperature. *Horticultural Plant Journal, 6*(4), 231–239, doi: 10.1016/j.hpj.2020.03.007.

Rezaeieh, K. A. P., Gurbuz, B., and Eivazi, A. (2016). Effects of different zinc levels on vegetative growth and essential oil contents of some Iranian and Turkish cumin (*Cumin cyminum* L.) genotypes. *Journal of Essential Oil Bearing Plants, 19*(5), 1181–1191, doi: 10.1080/0972060x.2016.1186573.

Rose, I., Biuković, G., Aderhold, P., Müller, V., Grüber, G., and Averhoff, B. (2011). Identification and characterization of a unique, zinc-containing transport ATPase essential for natural transformation in *Thermus thermophilus* HB27. *Extremophiles, 15*(2), 191–202, doi: 10.1007/s00792-010-0343-2.

Sawidis, T., Papadopoulou, A., and Voulgaropoulou, M. (2014). Effect of zinc on nectar secretion of *Hibiscus rosa-sinensis* L. *Protoplasma, 251*(3), 575–589, doi: 10.1007/s00709-013-0557-0.

Sharpley, M. S., and Hirst, J. (2006). The inhibition of mitochondrial complex I (NADH:ubiquinone oxidoreductase) by Zn^{2+}. *Journal of Biological Chemistry, 281*(46), 34803–34809, doi: 10.1074/jbc.M607389200

Shoaib, A., Ferdosi, M. F. H., Saleem, M. A., and Javed, S. (2021). Morphological and biochemical variations induced by synergy of salicylic acid and zinc in cockscomb. *Folia Horticulturae, 33*(1), 79–90, doi: 10.2478/fhort-2021-0006.

Srivastava, R. K., Rajpoot, R., Pandey, P., Rani, A., and Dubey, R. S. (2017). Cadmium alters mitochondrial membrane potential, inhibits electron transport chain activity and induces callose deposition in rice seedlings. *Journal of Plant Growth Regulation, 37*(1), 335–344, doi: 10.1007/s00344-017-9726-2.

Takahashi, K., Akaishi, E., Abe, Y., Ishikawa, R., Tanaka, S., Hosaka, K., and Kubohara, Y. (2003). Zinc inhibits calcineurin activity in vitro by competing with nickel. *Biochemical and Biophysical Research Communications, 307*(1), 64–68, doi: 10.1016/s0006-291x(03)01122-7.

van Schie, C. C., Haring, M. A., and Schuurink, R. C. (2006). Regulation of terpenoid and benzenoid production in flowers. *Current Opinion in Plant Biology, 9*(2), 203–208, doi: 10.1016/j.pbi.2006.01.001.

Vygodina, T. V., Zakirzianova, W., and Konstantinov, A. A. (2008). Inhibition of membrane-bound cytochrome c oxidase by zinc ions: high-affinity Zn^{2+}-binding site at the P-side of the membrane. *FEBS Letters, 582*(30), 4158–4162, doi: 10.1016/j.febslet.2008.11.018.

Yi, T., Wu, X., Long, Z., Duan, G., Wu, Z., Li, H., and Zhou, X. (2017). Overexpression of ubiquinol-cytochrome c reductase core protein 1 may protect H9c2 cardiac cells by binding with zinc. *BioMed Research International, 2017*, 1314297, doi: 10.1155/2017/1314297.

Yuan, Y., Yu, M., Zhang, B., Liu, X., and Zhang, J. (2019). Comparative nutritional characteristics of the three major Chinese *Dendrobium* species with different growth years. *PLoS One, 14*(9), e0222666, doi: 10.1371/journal.pone.0222666.

Zamiri, M. J., Mehrabi, R., Kavoosi, G. R., and Sharifabadi, H. R. (2017). Relationships between the activity of respiratory-chain complexes in pre-(biopsy) or post-slaughter muscle samples and feed efficiency in random-bred Ghezel lambs. *Animal Production Science, 57*(8), 1674, doi: 10.1071/an15184.

Zheng, S. G., Hu, Y. D., Zhao, R. X., Yan, S., Zhang, X. Q., Zhao, T. M., and Chun, Z. (2018). Genome-wide researches and applications on *Dendrobium*. *Planta, 248*(4), 769–784, doi: 10.1007/s00425-018-2960-4.

Zhou, C., Li, Z., Wiberley-Bradford, A. E., Weise, S. E., and Sharkey, T. D. (2013). Isopentenyl diphosphate and dimethylallyl diphosphate/isopentenyl diphosphate ratio measured with recombinant isopentenyl diphosphate isomerase and isoprene synthase. *Analytical Biochemistry, 440*(2), 130–136, doi: 10.1016/j.ab.2013.05.028.

Received: August 12, 2021; accepted: April 25, 2022

SUPPLEMENTARY MATERIALS

Table S1. Canonical correlation analysis between the activity of mitochondrial respiratory chain complexes and the production of precursors and ATP.

Correlations between Set-1 (the activity of mitochondrial respiratory chain complexes) and Set-2 (production of precursors and ATP)						
	IPP	DMAPP	Phe	LA	LNA	ATP
Complex I	0.7104	0.6786	0.7207	0.7872	0.6727	0.5994
Complex II	0.9404	0.9674	0.9549	0.9294	0.9483	0.9942
Complex III	0.5799	0.5574	0.6105	0.6911	0.5508	0.4600
Complex IV	0.6895	0.6677	0.7079	0.7787	0.6699	0.5780
Complex V	0.9549	0.9754	0.9643	0.9338	0.9534	0.9942
Canonical correlations						
0.999						
Test that remaining correlations are zero:						
Wilk's		Chi-SQ		DF		Sig.
0.000		51.362		30.000		0.009

IPP, isopentenyl pyrophosphate; DMAPP, dimethylallyl pyrophosphate; Phe, phenylalanine; LA, linoleic acid; LNA, linolenic acid; ATP, adenosine triphosphate; DF, degree of freedom.

Table S2. Canonical correlation analysis between the activity of mitochondrial respiratory chain complexes and emission of floral volatiles.

Correlations between Set-1 (the activity of mitochondrial respiratory chain complexes) and Set-2 (emission of floral volatiles)			
	Terpenoids	Benzoids	Fatty acid derivatives
Complex I	0.6595	0.4476	0.5092
Complex II	0.9692	0.9762	0.9915
Complex III	0.5268	0.3042	0.3576
Complex IV	0.6398	0.4167	0.4832
Complex V	0.9804	0.9706	0.9929
Canonical correlations			
0.999			
Test that remaining correlations are zero:			
Wilk's	Chi-SQ	DF	Sig.
0.000	60.329	15.000	0.000

DF, degree of freedom.

Table S3. Canonical correlation analysis between the production of precursors and ATP and emission of floral volatiles.

Correlations between Set-1 (the production of precursors and ATP) and Set-2 (emission of floral volatiles)							
	Terpenoids			Benzoids			Fatty acid derivatives
IPP	0.9905			0.8834			0.9420
DMAPP	0.9969			0.9262			0.9658
Phe	0.9837			0.8945			0.9446
LA	0.9696			0.8601			0.9096
LNA	0.9883			0.9012			0.9498
ATP	0.9856			0.9704			0.9919
Canonical correlations							
0.999							
Test that remaining correlations are zero:							
Wilk's	Chi-SQ	DF	Sig.	Wilk's	Chi-SQ	DF	Sig.
0.000	62.989	18.000	0.000	0.021	23.163	10.000	0.010

IPP, isopentenyl pyrophosphate; DMAPP, dimethylallyl pyrophosphate; Phe, phenylalanine; LA, linoleic acid; LNA, linolenic acid; ATP, adenosine triphosphate; DF, degree of freedom.

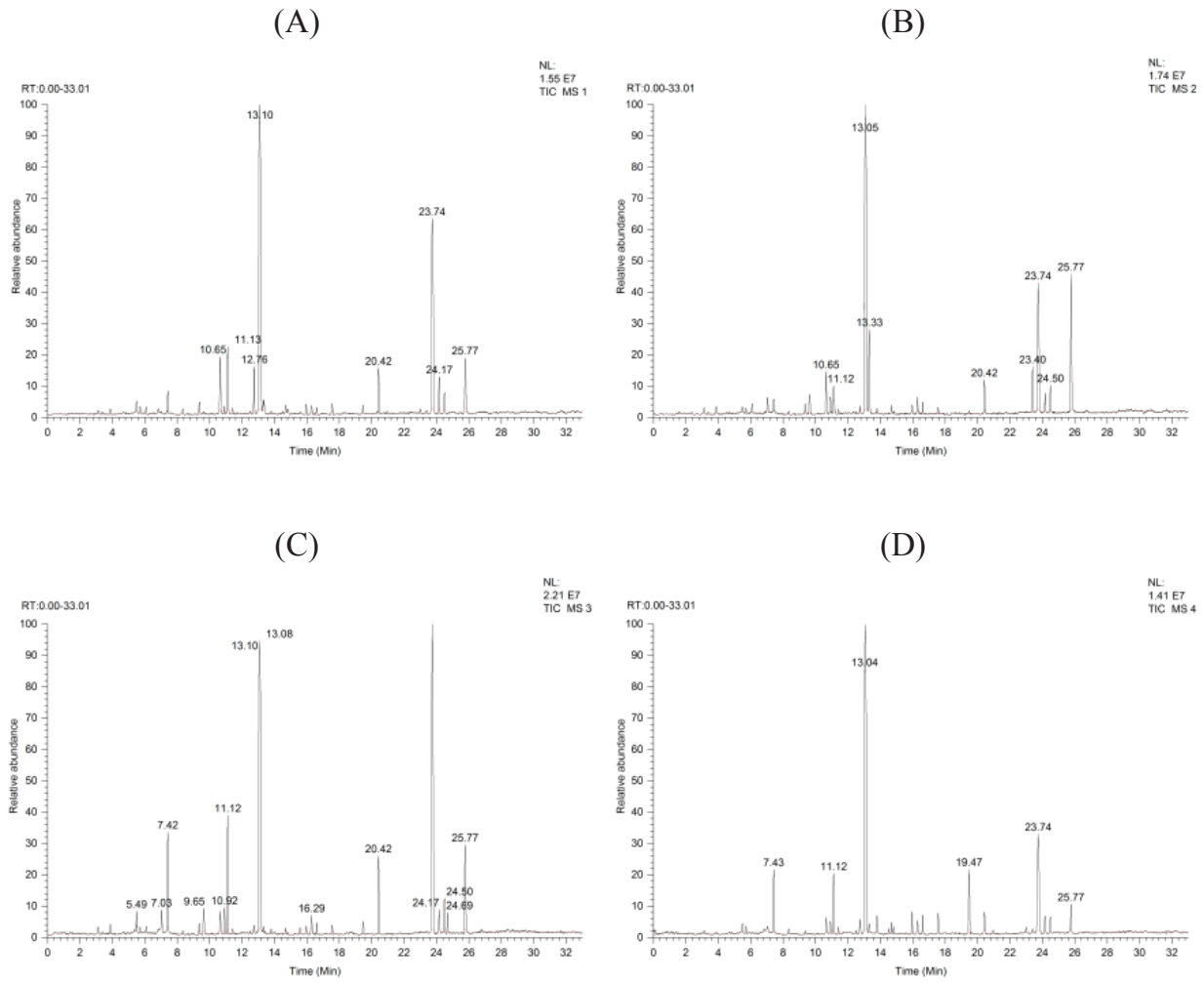

Figure S1. Total ion chromatogram [(A), the control group; (B), 2 mM $ZnSO_4$ treatments; (C), 4 mM $ZnSO_4$ treatments; (D), 8 mM $ZnSO_4$ treatments] of floral volatiles from *D. huoshanense* petals at 6 h after different $ZnSO_4$ concentration treatments. MS, mass spectrometer; TIC, total ion chromatograph; NL, nominal level; RT, retention time.

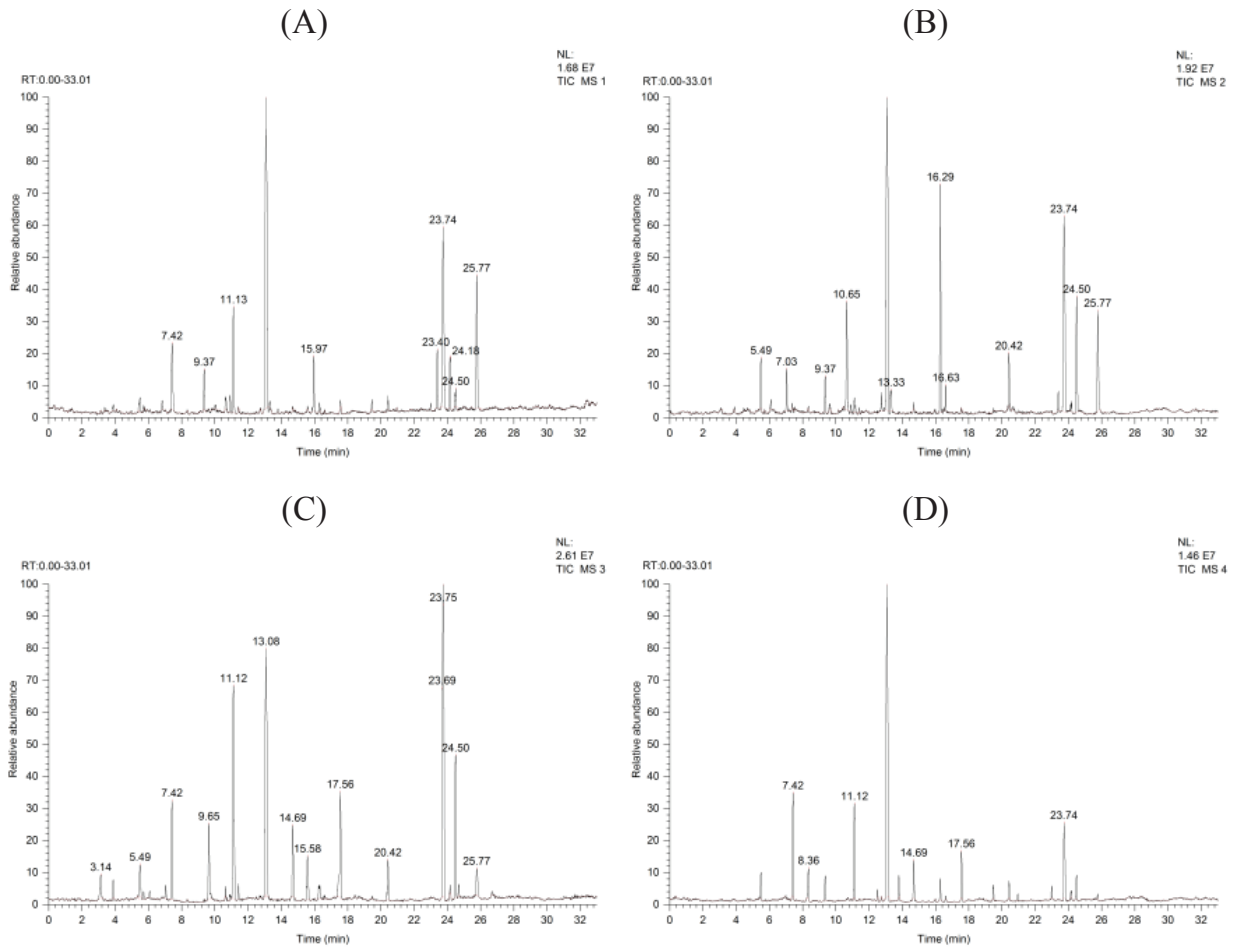

Figure S2. Total ion chromatogram [(A), the control group; (B), 2 mM $ZnSO_4$ treatments; (C), 4 mM $ZnSO_4$ treatments; (D), 8 mM $ZnSO_4$ treatments] of floral volatiles from *D. huoshanense* petals at 9 h after different $ZnSO_4$ concentration treatments. MS, mass spectrometer; TIC, total ion chromatograph; NL, nominal level; RT, retention time.

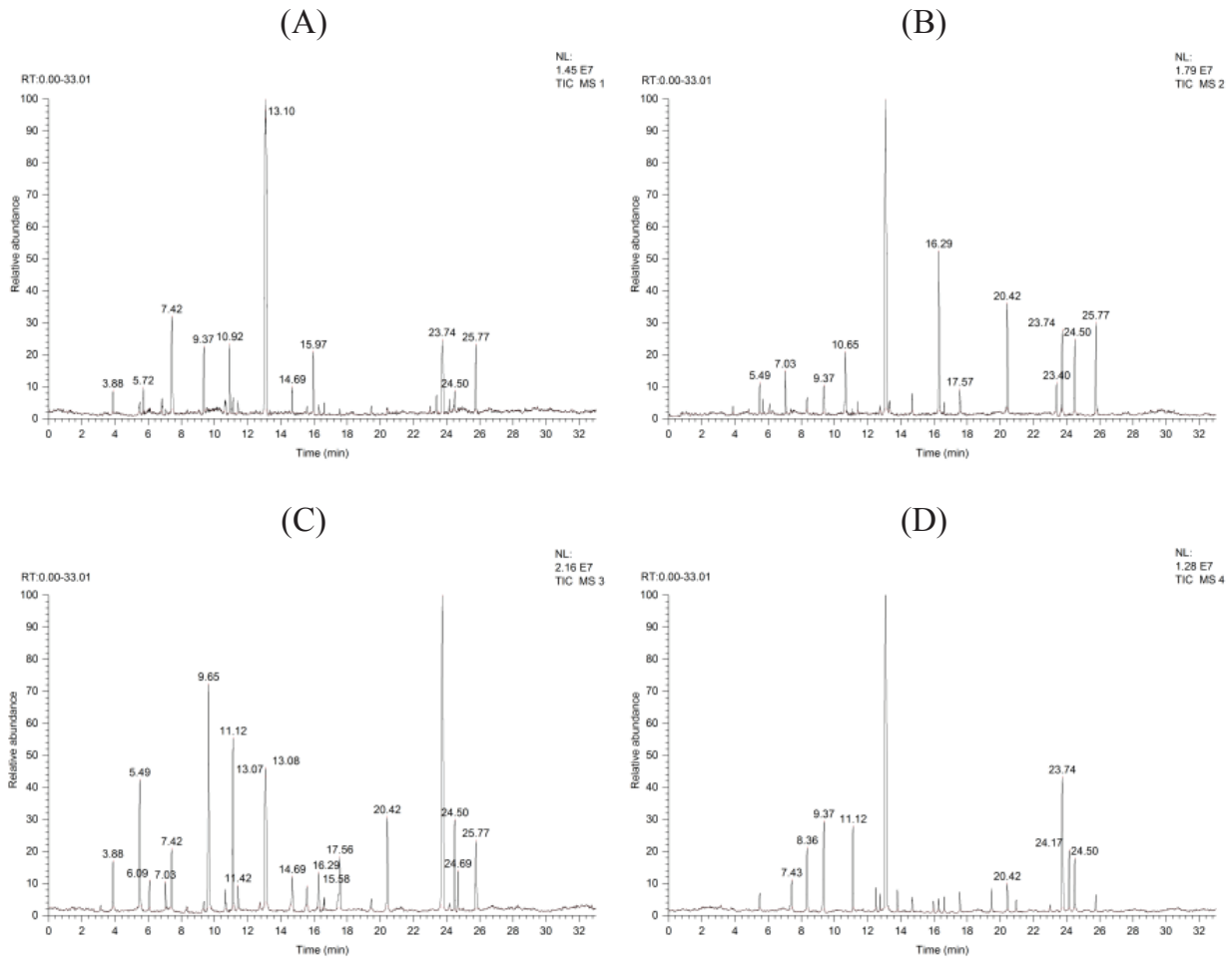

Figure S3. Total ion chromatogram [(A), the control group; (B), 2 mM $ZnSO_4$ treatments; (C), 4 mM $ZnSO_4$ treatments; (D), 8 mM $ZnSO_4$ treatments)] of floral volatiles from *D. huoshanense* petals at 12 h after different $ZnSO_4$ concentration treatments. MS, mass spectrometer; TIC, total ion chromatograph; NL, nominal level; RT, retention time.